The Sumatran Fault Zone—from Source to Hazard

Danny Hilman Natawidjaja

Journal of Earthquake and Tsunami

Journal of Earthquake and Tsunami, Vol. 1, No. 1 (2007) 21–47

World Scientific
www.worldscientific.com

THE SUMATRAN FAULT ZONE — FROM SOURCE TO HAZARD

DANNY HILMAN NATAWIDJAJA

Research Center for Geotechnology, Indonesian Institute of Sciences (LIPI)
LIPI – Bld.70, Sangkuriang Street, Bandung, 40135, Indonesia

WAHYU TRIYOSO

Department of Geophysics & Meteorology, Bandung Institute of Technology (ITB)
Ganesha Street, Bandung, Indonesia

The substantial portion of the dextral component of the Sumatran oblique convergence is accommodated by the Sumatran fault. This 1900 km-long active strike-slip fault zone runs along the backbone of Sumatra pose seismic and fault hazards to dense population on and around the fault zones. The Sumatran fault is highly segmented, and consists of 20 major geometrically defined segments, which range in length from about 60 to 200 km. These segment lengths influenced seismic source dimensions and have limited the magnitudes of large historical fault ruptures to between M_w 6.5 and about 7.7. Slip rates along the fault increase northwestward, from about 5 mm/yr around the Sunda Strait to 27 mm/yr around Toba Lake. These sliprate values provide a quantitative basis for calculation of average expected recurrence periods for large earthquakes on each segment. Deterministic and probabilistic hazard assessments are constructed based on these active fault data.

1. Introduction — Plate-Tectonic Environment

The island of Sumatra sits atop the Southeast Asian plate, which overrides the subducting Indian and Australian oceanic plates that converges obliquely at about 50 to 70 mm/yr [Prawirodirdjo *et al.*, 2000]. The oblique convergence is partitioned into two components: the dip slip is accommodated on the subduction interface, and the strike-slip component is accommodated largely by the Sumatran fault [McCaffrey, 1992; Sieh and Natawidjaja, 2000]. Other strike-slip faults that occur in similar settings include the left-lateral Philippine fault (which is parallel to the Luzon and Philippine trenches), the right-lateral Median Tectonic Line (which is parallel to the Nankai trough, Japan), and the Atacama fault (which lies parallel to the South American trench, offshore Chile).

The 1900 km long Sumatran fault zone (SFZ) traverses the back-bone of Sumatra, within or near the active volcanic arc. [Sieh and Natawidjaja, 2000]. At its northern terminus, the Great Sumatran fault zone transforms into the spreading centers of the Andaman Sea [Curray and others, 1979]. At its southern end, around the Sunda Strait, the fault curves southward toward and possibly

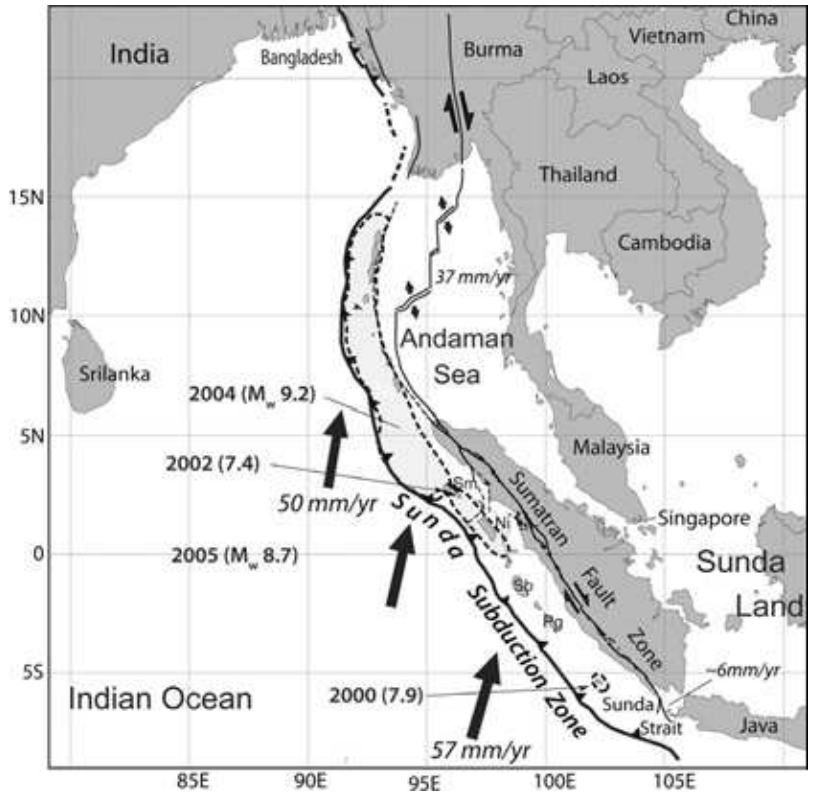

Fig. 1. The Great Sumatran fault zone is a trench-parallel, right-lateral strike-slip fault. It traverses the hanging-wall block of the Sunda trench from the Sunda Strait to the spreading centers of the Andaman Sea. Solid arrows relative plate motions from NUVEL-1 [Larson *et al.*, 1997]. Ellipsoids along the fore-arc regions are the seismic sources of the recent-megathrust earthquakes.

intersects the Sunda trench [Le Pichon *et al.*, 1981; Diament *et al.*, 1992; Sieh and Natawidjaja, 2000] (Fig. 1).

The Sumatran fault zone poses major hazards, particularly to the highly populated areas on and around the active fault trace. More than a dozens large earthquakes have occurred historically in the past 200 yeas. They caused great loss of life and property. However, until now this natural disaster threats have not been considered seriously for hazard-mitigation acts and for spatial planning and building codes.

2. Active Fault Mapping

The grossest features of the Sumatran fault have long been known from analysis of small-scale topographic and geologic maps [Katili and Hehuwat, 1967]. More detailed small-scale maps of the fault, based upon analysis of satellite imagery, have been produced more recently [Bellier *et al.*, 1997; Detourbet *et al.*, 1993].

The unavailability of stereographic imagery, however, limited the resolution and the reliability of these small-scale maps. To be of use in seismic hazard assessments the active fault map must be constructed on a scale that is large enough to clearly discriminate fault strands, changes in strike and structural discontinuities between strands.

Sieh and Natawidaja [2000] mapped the Sumatran fault zone based primarily upon inspection of its geomorphic expression on 1:50,000-scale topographic maps and 1:100,000-scale aerial photographs. These data were digitized and attributed, using the Geographic Information System (GIS) software. Geomorphic expression is especially reliable for mapping high slip rate faults, where tectonic landforms commonly develop and are maintained at rates that exceed local rates of erosion or burial [Yeats *et al.*, 1997, Chapter 8]. Examples of geomorphologically based regional maps of active faults include active fault maps of Japan, Turkey, China, Tibet, and Mongolia [Research Group for Active Faults, 1980; Saroglu *et al.*, 1992; Tapponnier and Molnar, 1977] as well as most maps of submarine active faults. However, the geomorphic expressions of active faults with slip rates that are lower than or nearly equal to local rates of erosion or burial is likely to be obscure. This is especially likely if the faults are short, have small cumulative offset, or have no component of vertical motion. Because of our reliance on geomorphic expression, their map of the Sumatran fault undoubtedly excludes many short, low-rate active fault strands. The 1:1,000,000 scale version of their map can be viewed and downloaded from http://www.tectonics.caltech.edu/sumatra/sumatranfault.htm. The SFZ is highly segmented. These fault segments are separated by more than a dozen discontinuities, ranging in width from $\sim$4 to 12 km [Sieh and Natawidjaja, 2000]. Theoretically, these discontinuities and bends in the fault are large enough to influence the seismic behavior of the fault [Harris *et al.*, 1991; Harris and Day, 1993]. In fact, the ends of historical earthquake ruptures along the SFZ seem to have been constrained by these large fault stepovers [e.g. Natawidjaja *et al.*, 1995].

Sieh and Natawidjaja [2000] divide the Sumatran fault into 20 major segments including Batee fault ranging in length from 35 km to 200 km (Fig. 2 and Table 1). For systematic and consistency, they named each segment by the name of a major river or bay along the segment. In older literatures, names of fault segments derived variously from nearby cities, districts, basins, and rivers. These include Banda Aceh Anu, Lam Teuba Baro, Reuengeuet Blangkejeren, Kla-Alas, Ulu-Aer, Batang-Gadis, Kepahiang-Makakau, Ketahun, Muara Labuh, and Semangko [e.g., see Katili and Hehuwat, 1967; Cameron *et al.*, 1983; Durham, 1940]. Sieh and Natawidjaja [2000] also mapped an active thrust fold belt called the Toru active thrust-fold belt west of SFZ around the 1N latitude (Fig. 2).

Historical earthquake records along the Sumatran fault suggest that fault stepovers constrained past fault ruptures and hence are likely to govern future rupture dimensions. An excellent example is mechanisms of the 1926 and 1943 events in west Sumatra (Fig. 3). The 1926 event is a double-mainshock event. The first shock ruptured the segment between Dibawah and Singkarak lakes. Then, about

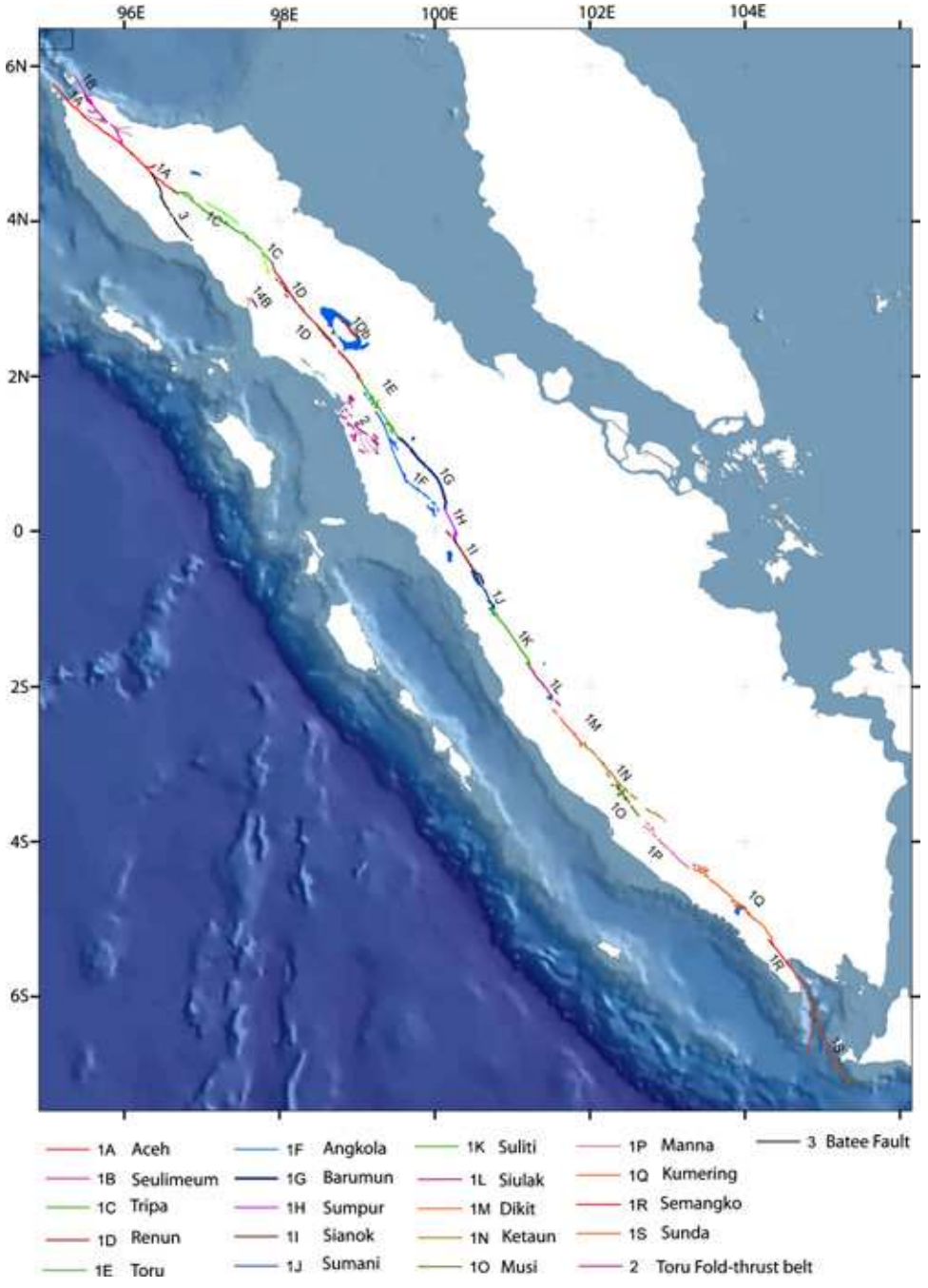

Fig. 2. This map of the principal active traces of the Sumatran fault zon (SFZ) is based upon interpretation of 1:100,000 stereographic aerial photographs and 1:50,000 topographic maps. The SFZ can be divided into 20 fault segments. Ends of segments are mostly major fault stepovers of 4 km-width or more of separations.

Table 1. Fault Segmentation of the Sumatran Fault Zone that controls terminations of earthquake ruptures [modified from Sieh and Natawidjaja,[2000].

	Section	Index #	Location Y1	Location Y2	Length (km)	Historical Earthquakes Year(M)	Geomorphic Features	Magnitude M^1_{Max}	Magnitude M^2_{Max}	Slip Rate by Geol. mm/yr	Slip Rate by GPS mm/yr
1	Sunda	1S	−6.75	−5.9	150	None - but many recent M4-6	submarine graben	7.6	7.7	n/a	n/a
2	Semangko	1R	−5.9	−5.25	65	1908	east facing scarp	7.2	7.2	n/a	n/a
3	Kumering	1Q	−5.3	−4.35	150	1933(Ms = 7.5); 1994(Mw = 7.0)	Suoh geo thermal valley	7.6	7.7	n/a	n/a
4	Manna	1P	−4.35	−3.8	85	1893	mountainous range on east side of the fault	7.3	7.4	n/a	n/a
5	Musi	1O	−3.65	−3.25	70	1979(Ms = 6.6)	valley, depression	7.2	7.3	11	n/a
6	Ketaun	1N	−3.35	−2.75	85	1943(Ms = 7.3); 1952(Ms = 6.8)	depression valley and Kaba volcano	7.3	7.4	11	n/a
7	Dikit	1M	−2.5	−2.4	60	no record	n/a	7.2	7.2	11	n/a
8	Siulak	1L	−2.25	−1.7	70	1909(Ms = 7.6); 1995(Mw = 7.0)	Lake Kerinci and Kunyit volcano	7.2	7.3	11	23
9	Suliti	1K	−1.75	−1	95	1943(Ms = 7.4)	small depression, calderas and young volcanic cone	7.4	7.4	11	23 ± 5
10	Sumani	1J	−1	−0.5	60	1943(Ms = 7.6); 1926(Ms $\sim$ 7)	Lake Diatas, calderas and Talang volcano	7.2	7.2	11	23
11	Sianok	1I	−0.7	0.1	90	1926 (Ms $\sim$ 7)	Lake Singkarak	7.3	7.4	11	23 ± 3
12	Sumpur	1H	0	0.3	35	no record	wide depression associated with normal faults	6.9	6.9	n/a	n/a
13	Barumun	1G	0.3	1.2	125	no record	long (Sumpur) valley along the fault	7.5	7.6	n/a	4
14	Angkola	1F	0.3	1.8	160	1892(Ms = 7.7)	mountainous ranges on both sides of the fault	7.6	7.7	n/a	19 ± 4
15	Toru	1E	1.2	2	95	1987(Ms = 6.6)	uplifted hill on the east side of the bend	7.4	7.4	n/a	24
16	Renun	1D	2	3.5	220	1916; 1921 (mb = 6.8); 1936(Ms = 7.2)	Tarutung Valley	7.8	7.9	27	26 ± 2
17	Tripa	1C	3.4	4.4	180	1936 (Ms7.2); 1990(Ms = 6?)	Alas Valley	7.7	7.8	n/a	n/a
18	Aceh	1A	4.4	5.4	200	no record	mountainous range, associated with thrusts	7.7	7.9	n/a	n/a
19	Seulimeum	1B	5	5.9	120	1964(Ms = 6.5)	Small depression on dilatational stepover	7.5	7.6	n/a	13

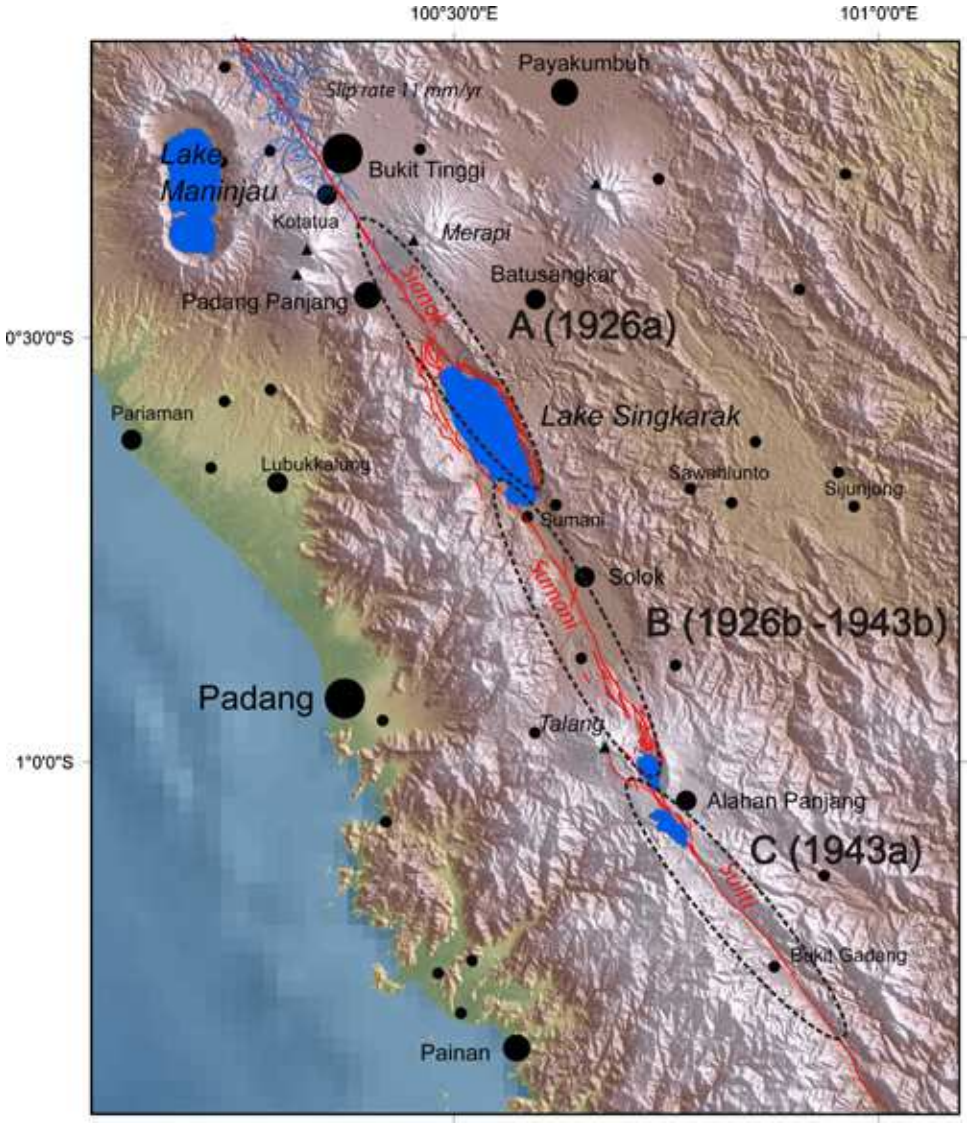

Fig. 3. Fault discontinuities controlled seismic sources of the 1926 and 1943 events in west Sumatra. The 1926 and the 1943 events are the double- mainshock events. The first shocks in 1926 ruptured the Sumani segment that is terminated by large stepovers in Singkarak and Dibawah-Diatas lakes. After a pause about half an hour, the second shock ruptured the Sianok segment north of Singkarak Lake. The 1943 first shock ruptured the Suliti segment south of Diatas Lake. The second shock, 4 hour later, ruptured the Sumani segment [after Natawidjaja *et al.*, 1995].

half an hour later, the second shock ruptured the segment north of Singkarak Lake. Interestingly, the 1943 event is also the double-mainshock event. The first shock ruptured tens of kilometers of the segment south of Diatas Lake, causing significant destructions in the town of Alahan Panjang [Natawidjaja *et al.*, 1995]. Then about

four hours later, the second shock demolished Alahan Panjang and caused heavy destructions to areas along the fault segment between Diatas and Singkarak lakes.

3. Slip Rates

The combination of an arcuate plate boundary and a distant pole of rotation suggests that the rate of dextral slip along the Sumatran fault increases northwestward [e.g. Fitch, 1971; McCaffrey, 1991; Prawirodirdjo, 2000; Sieh and Natawidjaja, 2000] (Fig. 1). McCaffrey (1991) calculated hypothetical trench-parallel extension rates for the block between the trench and the GSF. If one assumes that the extension rate is uniform along the entire Sumatran arc and that all of this extension is accomodated by slip on the SFZ, then the fault's slip rate should increase from near zero at the Sunda Strait to about 4 cm/yr at the northern tip of Sumatra.

Observations near the northwestern and southeastern termini of the GSF support this contention (Fig. 1). Curray and others (1979) showed that the rate of opening across the spreading centers of the Andaman Sea has averaged about 37 mm/yr for the past 11 million years (Fig. 1). They had proposed that most of this motion is carried to the southeast by the SFZ. The slip rate inferred for the SFZ near its southern terminus, however, is far lower. Diament and others (1992) propose that the rate there is 10 mm/yr or less. Natawidjaja [1997] and Harjono and Natawidjaja [2003] had calculated the rate of opening across the major fault graben at the fault zone's southern end to be about 2.5 mm/yr perpendicular to the graben since 5 Ma, based on the total amount of fault's horizontal displacements (i.e. throw) from re-analyzing the seismic-reflection profiles of Lassal *et al.* [1989].

We have determined geological slip rates at three selected sites (Fig. 4) in order to place additional quantitative constraints on the kinematics of the region. The geological-slip-rate determinations are relatively easy in Sumatra because river channels and offset along the Sumatran fault had incised many thick mono-age pyroclastic deposits. The results suggested that dextral slip rates do increase northward, as expected, but not uniformly (Fig. 4). Geological slip rates along the fault segments south of the Equator are approximately 11 mm/yr. North of Equator, they increase to 27 mm/yr at 2°N [Sieh *et al.*, 1991, 1994; Sieh and Natawidjaja *et al.*, 2000].

Genrich and others [2000] conducted several transects of survey-mode GPS measurements in order to determine the modern sliprates. The GPS sliprate for the fault segment around the Toba Lake ($\sim 2°$N) is 26 ± 2 mm/yr, which is consistent with the 27 mm/year of the geological slip rate (Fig. 4). In contrast, the GPS sliprate at around 0.5°S is about 23 mm/yr, which is twice as much as the geologically-determined sliprate. This discrepancy needs to be investigated further. The GPS-survey-mode measurement across the Sumatran fault in North Sumatra yielded the sliprate of less than 13 mm/yr [Genrich *et al.*, 2000]. The result of this GPS survey, unfortunately, has large uncertainties. Nonetheless, this low sliprate contradicts the hypothesis of the increasing sliprate toward the Andaman Spreading

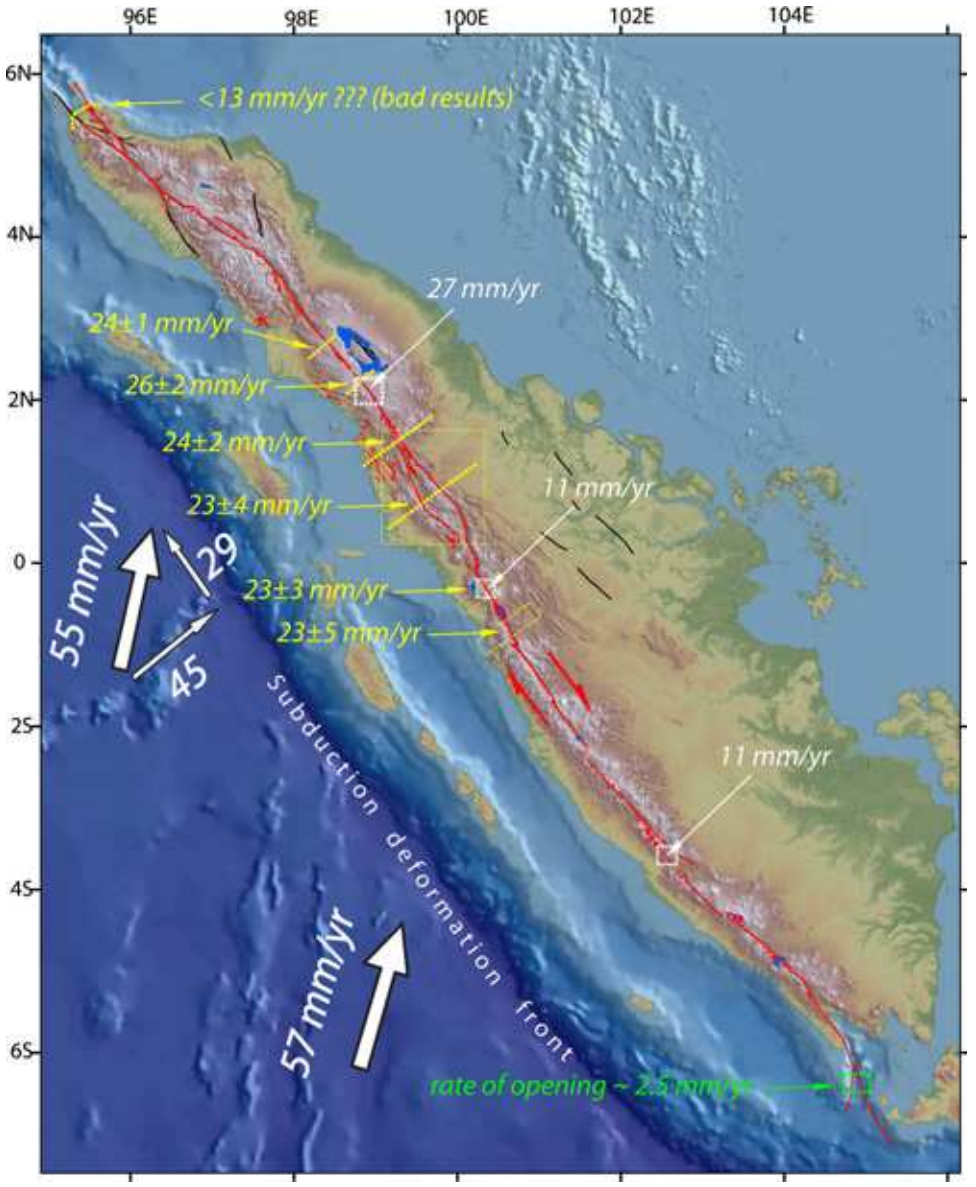

Fig. 4. Map showing fault sliprates along the SFZ. The velocity values (mm/yr) in white are the geological sliprates [Sieh *et al.*, 1991, 1994]. The values in yellows are the sliprates from the GPS survey-mode measurements [from Genrich *et al.*, 2000]. The trench-parallel component of the plate convergence is about 29 mm/yr, and is taken to a large extent by the dextral movement along the SFZ. The sliprate increases northward, but it is not uniform. The southern half of the fault moves about 11 mm/yr. From about 0.5°S to 2°N, it increases to 27 mm/yr. Mainly based on poor-quality GPS survey in the Aceh region, it may be evidence that from 2°N to 6°N sliprate decreases significantly.

Center. Curray and others [1979] suggested that the west-Andaman fault (WAF), located west of North Sumatra, is an active structure, thus also playing a significant role in this region. Recent marine cruise conducted by the UK team lead by Satish Singh [*Pers.Comm.*] found clear evidences of fresh-morphotectonic features along WAF, which suggests that this fault is probably highly active. Hence, the decreasing sliprate along the Sumatran fault, from 2°N to 6°N may be related to the existence of WAF. In otherworld, we may speculate that the trench–parallel slip component on this latitude is taken to a large extent by the West-Andaman fault. Further investigation is required indeed, to solve this interesting phenomenon.

4. Historical and Recent Seismicity

Documenting past ruptures is the first-crucial step to evaluate future seismic potentials. However, gathering these data is not easy because most of these occurred tens or even more than a hundred years ago, so available data are sparse and not easy to collect, and most of them were not well documented in the past. Several historical earthquakes however have relatively well documentations as follows. *Reid* [1913] used geodetic measurements from before and after the 1892 Sumatran earthquake as support for his concept of elastic rebound. Berlage [1934] described the effects of the 1933 earthquake in south Sumatra. Visser [1927] described the effects of the 1926 Padangpanjang earthquake in west Sumatra. Untung *et al.*, [1985] conducted field investigations to document the 1943 event's rupture and fault offsets. Natawidjaja *et al.*, [1995] re-investigated field evidence of the 1926 and 1943 ruptures and interviewed the eye witnesses that are still alive and lived in the villages around the fault trace. Widiwijayanti *et al.*, [1996] conducted study on aftershocks of the Liwa 1994 earthquake (M_w 6.8). The summary of the documented historical fault ruptures is shown in Fig. 5. Future studies may be able to collect more comprehensive data of historical notes from various sources both inside and outside Indonesian literatures.

The SFZ, with sliprates ranges from 10 to 27 mm/yr, is classified as a highly active fault. We roughly estimated the frequency of earthquake occurrences along SFZ by calculating rate of seismic moment accumulation of each segment for given periods (Table 2). We intrapolate/extrapolate the values of known sliprate to other fault segments. We assume a fixed depth of a seismogenic zone at 15 km. We then calculate moment magnitudes for 100 yr and 200 yr return period (Table 2). The results show that in average, every 100 years of the accumulated strains in each segments of the SFZ are equivalent to earthquake from M_w 7.2 to 7.4. For 200 years return period, each segment of the SFZ is capable of generating earthquake with a magnitude range from M_w 7.4 to M_w 7.7. Thus, considering the SFZ consists of 19 or 20 fault segments, then we can conclude that the occurrence of earthquake with magnitude M_w 7.2–7.4 is about 2 events in every decade, and the occurrence of earthquake with magnitude M_w 7.4–7.7 is about 1 event in every decade. Note that we are assuming all the fault zones are entirely locked (= 100% seismic) from

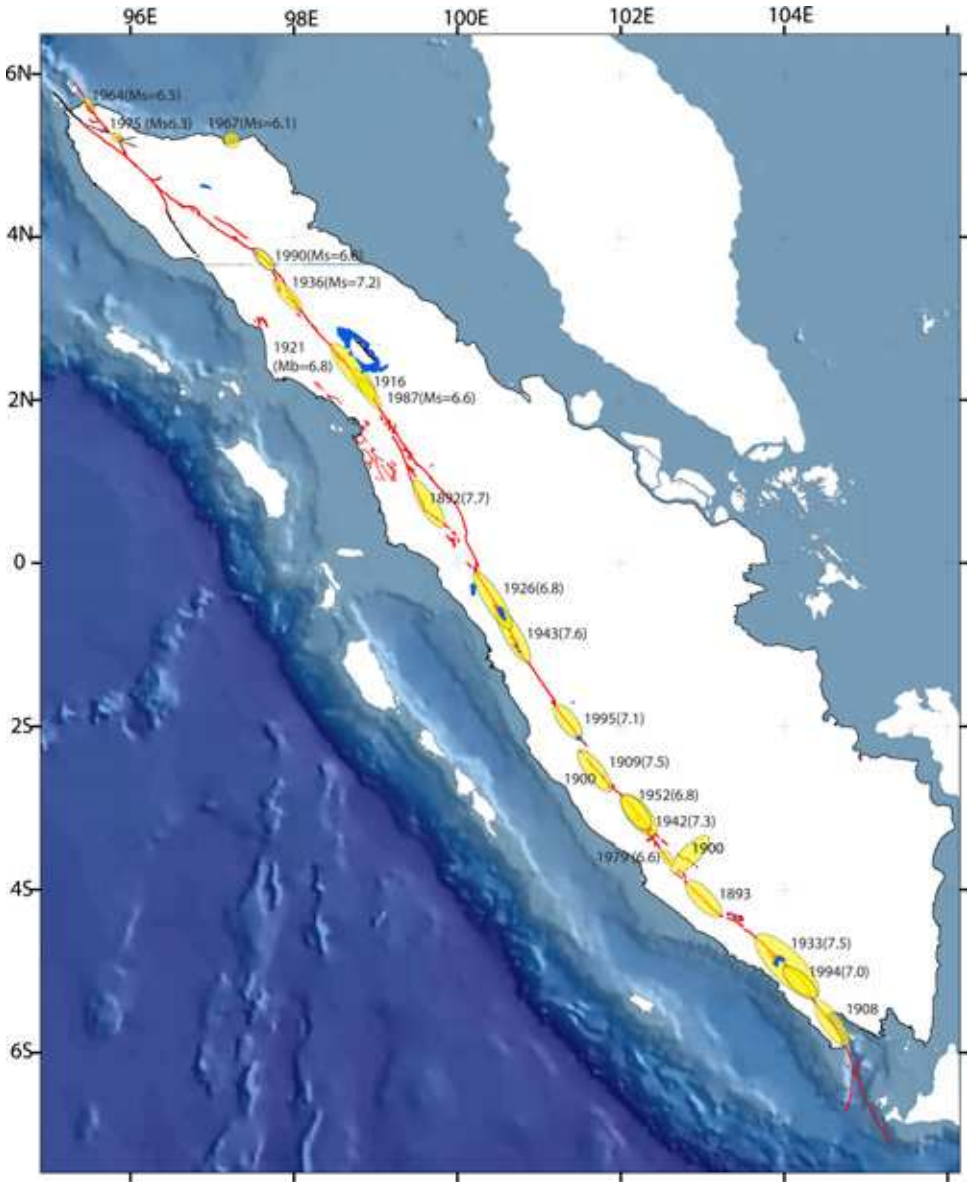

Fig. 5. Historical major earthquakes along the SFZ since 1892. The ellipsoids indicate fault segments that were ruptured during the earthquakes. Numbers indicate years of occurrences and number in brackets are earthquake magnitudes.

Table 2. Estimation of rates of seismic moment accumulations on each SFZ's segments for the 100 years and 200 years return period. The depth of seismic zone (D) is assumed at 15 km fixed depth. Mo (seismic moment) $= \mu * (\mathrm{L} * \mathrm{D})\,\mathrm{cm}^2 * \mathrm{S}\,\mathrm{cm}$; where $\mu = 3 * 10\,\mathrm{dyne/cm}^2$. S (accumulated slip) = Sliprate $*$ return period. M_w (moment magnitude) = (Log Mo $-$ 16.05)/1.5 (Hanks and Kanamori, 1979).

No	Segment	L (km)	Sliprate (cm/yr)	Slip Accumulation (cm)		100 Yr– Return Period		200 Yr– Return Period	
				100yr	200yr	Mo-100	Mw-100	Mo-200	Mw-200
1	Sunda	150	1	10	20	6.75E + 25	7.2	1.35E + 26	7.4
2	Semangko	65	1	10	20	6.75E + 25	7.2	1.35E + 26	7.4
3	Kumering	150	1	10	20	6.75E + 25	7.2	1.35E + 26	7.4
4	Manna	85	1	10	20	6.75E + 25	7.2	1.35E + 26	7.4
5	Musi	70	1	10	20	6.75E + 25	7.2	1.35E + 26	7.4
6	Ketaun	85	1	10	20	6.75E + 25	7.2	1.35E + 26	7.4
7	Dikit	60	1	10	20	6.75E + 25	7.2	1.35E + 26	7.4
8	Siulak	70	1	10	20	6.75E + 25	7.2	1.35E + 26	7.4
9	Suliti	95	1	10	20	6.75E + 25	7.2	1.35E + 26	7.4
10	Sumani	60	1	10	20	6.75E + 25	7.2	1.35E + 26	7.4
11	Sianok	90	1	10	20	6.75E + 25	7.2	1.35E + 26	7.4
12	Sumpur	35	1	10	20	6.75E + 25	7.2	1.35E + 26	7.4
13	Barumun	125	1	10	20	6.75E + 25	7.2	1.35E + 26	7.4
14	Angkola	160	1	10	20	6.75E + 25	7.2	1.35E + 26	7.4
15	Toru	95	2.7	27	54	1.82E + 26	7.5	3.65E + 26	7.7
16	Renun	220	2.7	27	54	1.82E + 26	7.5	3.65E + 26	7.7
17	Tripa	180	2.7	27	54	1.82E + 26	7.5	3.65E + 26	7.7
18	Aceh	200	1	10	20	6.75E + 25	7.2	1.35E + 26	7.4
19	Seulimeum	120	1	10	20	6.75E + 25	7.2	1.35E + 26	7.4

the ground surface to 15 km depth. So, this calculation estimates a maximum production of earthquakes.

The historical accounts of earthquake occurrence support this estimation. Since 1890, about 21 major earthquakes ruptured the segments of the SFZ with magnitudes ranges from 6.5 to 7.7 (Fig. 5). Thus, on average, the repetition of major earthquakes along the entire Sumatran fault is about one or two major earthquakes in every decade. Most of them occurred in highly populated regions, so they caused many casualties and great economic losses. Recent earthquakes occurred in south Sumatra in 1994 (M_w 7.0) and around Mount Kerinci in central Sumatra in 1995 (M_w 7.1).

Earthquake-hazard evaluations needs knowledge of last major earthquake events on the faults since this tells us about how much seismic energy has accrued in the *elapsed time.* For example, we take about 100 yr elapsed time as a threshold to generally assign the fault segments that now have capability of generating

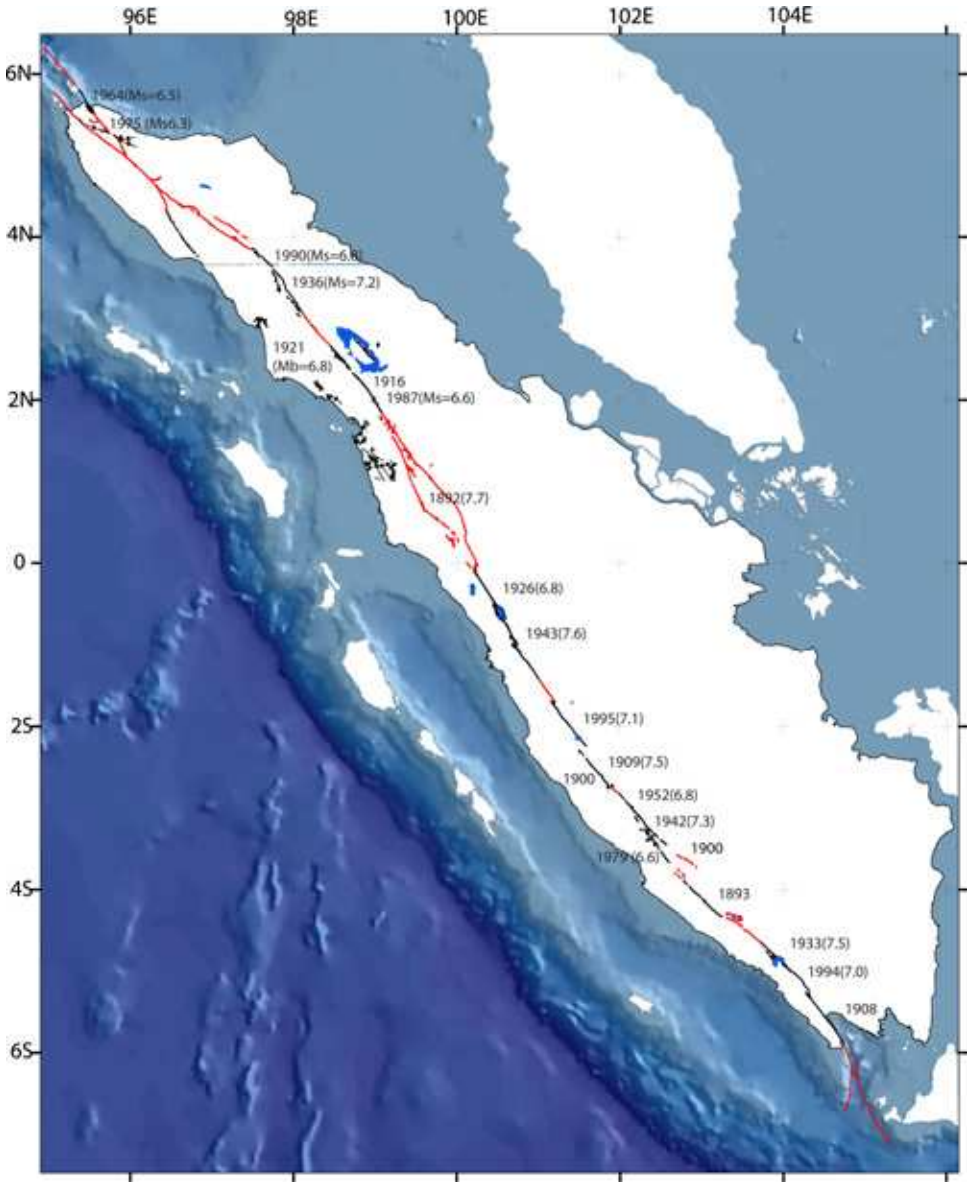

Fig. 6. Map showing the unbroken fault segments in the last century denoted by dark gray color code segments.

future destructive earthquakes. Figure 6 summarizes which segments have not ruptured in the past 100 years. The total length of these unbroken segments is about 1000 km, which includes a 325 km and 70 km long Banda Aceh and Seulimeum fault segments.

5. Fault and Seismic Hazards

Damaging effects caused by on-land earthquakes can be classified into two categories: primary and secondary effects. Primary effects are hazards associated with surface faulting and earthquake ground motion. Secondary effects include landslides and liquefactions triggered by the ground motions. Since earthquake sources lie in the bottom of the ocean floor, an earthquake event may excite tsunami. In earthquake-hazard-assessments, the primary earthquake hazards are usually considered first. The effects of surface faulting and ground shaking did cause largest parts of damages in some events, such as those occurred during the Chi-chi 1999 Taiwan earthquake (M_w 7.6) and recent Iran earthquake in 2003 (M_w 6.7). Another example from the subduction earthquake is of the great Alaskan earthquake (M_w 9.2), where the direct effects of shaking caused the greatest damages [Yeats *et al.*, Chapter 15, 1997].

However, it is not uncommon that secondary effects of some major earthquakes in the world caused far greater loss of life and property than their primary effects. For example, more than 100,000 people were killed by massive landslides triggered by the great 1920 earthquake (M = 8.7) in China [Close and McCormic, 1922], and during the 1970 Peruvian earthquake (M = 7.9), the ground motion triggered massive debris avalanche that killed more than 15,000 people in one city alone [Plafker *et al.*, 1971]. For the sub-marine earthquake, large tsunamis generated by ocean floor uplift commonly caused much greater loss of life and property than their ground motions, such as that occurred during the recent Aceh-Andaman 2004 earthquake, when its tsunami killed more than 250,000 people.

The most common earthquake-hazard assessments is the ground-motion assessment, which becomes of similar term to *the seismic hazard assessment*, and the most common risk assessment is the structural damages that result from this ground shaking or ground motion. This type of seismic hazard is commonly a necessary procedure, especially in developing critical structures such as major dams and nuclear power plants, where public interest is high and where licensing standards are very demanding. In the next section, we will discuss to some extent about the seismic hazard assessments of the Sumatran fault system since this is the most familiar aspect to engineers, planners, and general public. In doing so, we would like to emphasize that it would be a mistake to assume that seismic or more exactly ground-motion hazard assessment is the ultimate goal of every hazard assessment project.

The house and engineering constructions, even if they have appropriate *seismic-proof* (*i.e. shaking-resistant*) design, can still be damaged by earthquake event if there are located right on surface fault ruptures, or even if they are not right on the rupture zone, may still be damaged and collapsed by sudden co-seismic movements around or above the earthquake faulting as observed in some earthquake events around the world, not because of the effects of earthquake's ground accelerations [Paul Burton, pers. comm, 2006].

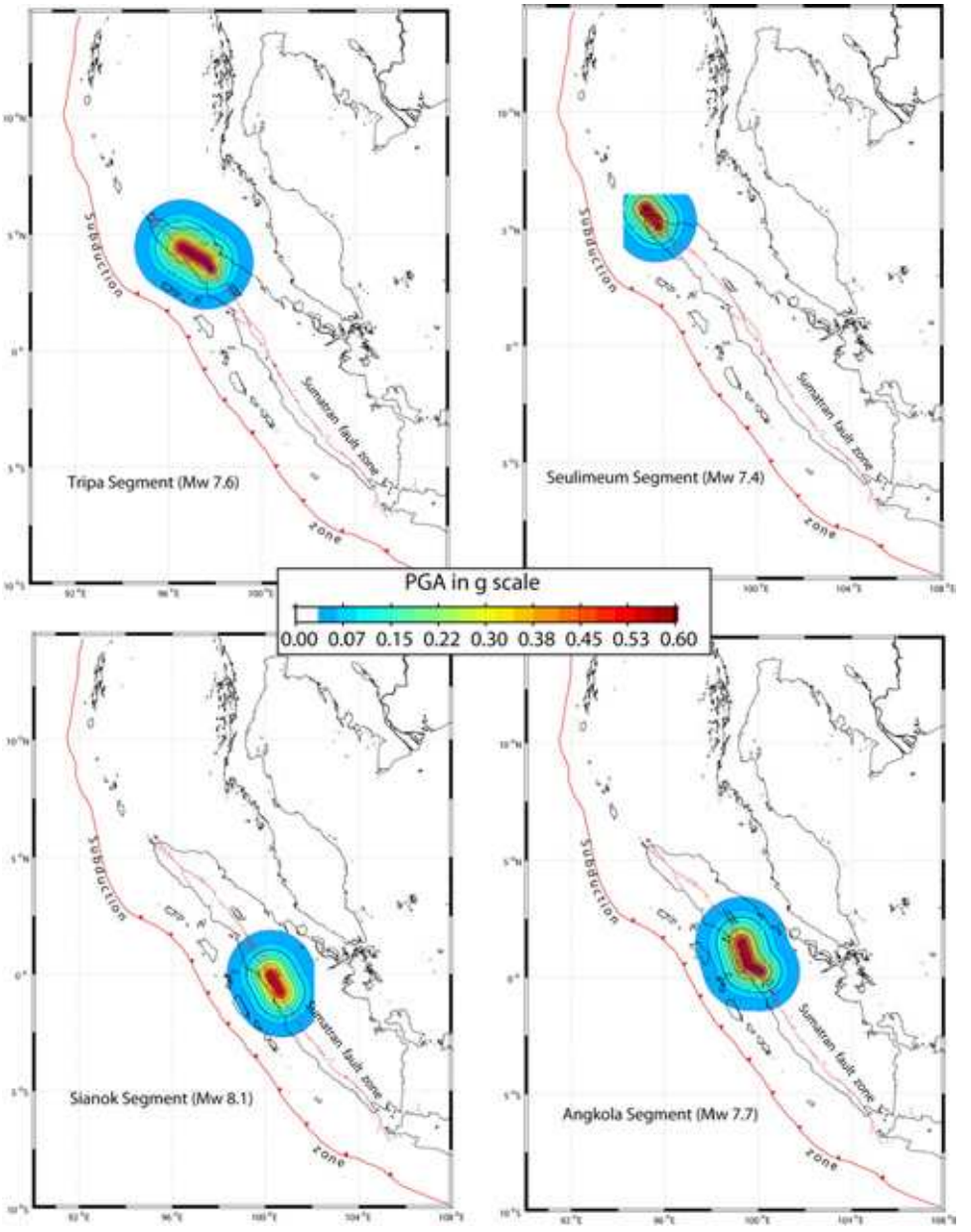

Fig. 7. Deterministic Seismic Hazard Assesments (DSHA). Maps of expected peak ground accelerations (PGA) of the maximum credible earthquake (MCE) on several fault section of SFZ using empirical relation equations of Fukushima and Tanaka [1990].

Thus, to delineate hazards associated with earthquake's surface faulting, detailed maps of active faults with their sliprates and their historical seismicity, such as shown in Figs. 2, 4 and 5, are also considered as a simple type of earthquake-hazard assessment products. It is now a common practice that the areas along active fault strands are specifically regulated to mitigate earthquake-faulting hazards, such as the application of the Alquist-Priolo acts to active fault zones in California [http://www.consrv.ca.gov/cgs/rghm/ap/index.htm]. In general, houses and especially large-public buildings should not build on or near highly-active fault strands.

However, one should not assume that area on and near any active fault is always dangerous, but it depends on *degree of earthquake- hazard potential* of the faults. We define earthquake-hazard potential as a likelihood of potential hazards from a future destructive earthquake on a certain fault segment. The basics to evaluate earthquake-hazard potential, is to have appropriate data on fault segmentations that determine the *maximum credible earthquake* (MCE) [e.g. Yeats *et al.*, 1997, Chapter 15], fault sliprates, and past (historical) ruptures, such as illustrated in Figs. 3, 4 and 5. In some portion along the fault, the fault movements may be *aseismic*, so they do not accumulate large strain accumulation. In this case, even the sliprate is high but the movement is accommodated by creeping, so that area would not likely to produce large earthquake.

5.1. *Seismic hazard assesments*

The seismic hazard or more exactly ground-motion hazard is a measure of ground shaking associated with earthquake(s) and is defined at any location of a certain level of ground shaking. A map of seismic hazard is usually expressed in terms of ground shaking parameters such as intensity, peak ground acceleration, velocity, or probability of certain ground motion. Seismic hazard assessment is a first step leading to seismic risk assessment. Seismic risk can be evaluated by convolving seismic hazard with a risk function of artificial constructions such as houses, buildings, infrastructures, of population, and so on.

There are two different approaches in Seismic Hazard Study and Analysis. The first method is the deterministic approach or deterministic seismic hazard assessment (DSHA). The second method is the probabilistic approach or the probabilistic seismic hazard assessments (PSHA). The two methods have each purpose. The DSHA is quite useful to estimate possible range value of shaking and its correlation with building or construction's strength. The PSHA is useful to adjust a level of seismic hazard with a lifetime of a specified construction. In both methods, comprehensive and accurate data of active faults and earthquake source parameters is essential. The fault and source parameters include fault segmentations and their characteristic magnitudes, fault sliprates, recurrence intervals, and historical past ruptures.

The DSHA takes into account probability of range values of shaking in term of Peak Ground Acceleration (PGA), velocity (PGV), or displacement at a site due to a specified seismic source in the vicinity. To estimate a possible ground motion due to an earthquake event, a certain attenuation relationship is used. Attenuation relationship is a function of an earthquake magnitude, a distance of an earthquake event to the site, and geological condition along seismic path and at and around the site. This quality of the results depends on how precise our assumption in identifying the MCE and the reliability of attenuation function. The PSHA is usually applied for the aim of estimating probable annual shaking as the sum of probability of each rate function of each specified seismic source around the site. The DSHA has the advantage that it does not require the presence of data bearing on time-dependent processes such as rate of earthquake occurrence or fault sliprate. This assessment simply considers the *credible* worst-case scenario.

Probabilistic approaches, however, are becoming more commonplace, usually resulting in maps portraying the likelihood of earthquake occurrences or of specific parameters, such as probability of exceedance of peak ground acceleration (PGA) or velocity (PGV) during a specified time [Yeats *et al.*, 1997, Chapter 15]. PSHA involves three steps: 1. Specification of the seismic-source models, 2. Specification of the ground-motion model (i.e. attenuation relationship(s), and 3. the probabilistic approaches. The probabilistic approaches are basically mathematical procedures to sum-up the contribution of all seismic sources to the shaking level in certain sites/areas for certain period of time.

For the exercise, we apply the Fukushima and Tanaka [1990] attenuation relationship to estimate PGA (Peak Ground Acceleration). We use this attenuation relationship considering that the Sumatran seismo-tectonic environment is almost similar to that of Japan. Base on physical characteristics of an earthquake source, Fukushima and Tanaka [1990] consider the saturation of acceleration amplitude in a near-source region whose extent depends on the size of the earthquake. The model should also have attenuation characteristics of a simple point source with geometric spreading effect in the middle to the far field. Considering the above aspects, they proposed the attenuation relationship for PGA as the following,

$$\log_{10} \mathrm{A} = 0.41 M_{\mathrm{w}} - \log_{10}(\mathrm{R} + 0.032.10^{0.41 M_{\mathrm{w}}}) - 0.0034\mathrm{R} + 1.30$$

(Fukushima and Tanaka, 1990)

in which, A is the mean of the peak acceleration from the two horizontal components at each site (cm.sec^{-2}), R is the shortest distance between the site and the fault rupture (km), and M_{w} is the moment magnitude.

The Fukushima and Tanaka attenuation relationship [1992] was also used by the GSHAP (Global seismic Hazard Assessment Program) for Indonesia and Malaysia. Petersen *et al.* [2004] found that this attenuation relationships are reliable to have been applied for the site up to 500 km away from the seismic sources of the subduction-zone type, while the attenuation relationships of Young *et al.*, [1997] gives inconsistent values for sites more than 200 km distant. For the intraplate

earthquake sources like the Sumatran fault zone, Megawati and others (2003) found that Fukushima and Tanaka attenuation relations well fit the simulated ground-motion data from the synthetic-seismogram analysis, at least for the site–seismic source distance less than 400 km.

5.2. *Results of deterministic seismic hazard assesments of SFZ*

Based on fault segmentation and source parameters described in Table 1 and Fig. 2, we analyze the expected ground motion level in term of peak ground acceleration (PGA) from the MCE of each fault segment using the attenuation relationships of Fukushima and Tanaka [1990], described above. Examples of the results are shown in Fig. 10. In general, the results indicate that earthquakes with magnitude ~ 7 gives PGA > 0.3 or PGA > 0.5 in areas less than 45 km or less than 10 km in distance from the fault zone respectively.

5.3. *Probabilistic seismic hazard evaluation*

The annual exceedance probability of peak horizontal ground acceleration (PGA) u at a site due to events at a particular cell k under the Poisson distribution is given by:

$$P(u \geq u_0) = P_k(m \geq m(u_0, D_k)) = 1 - e^{(-v_i(\geq m(u_0, D_k)))} \tag{1}$$

where $P_k(m \geq m(u_o, D_k))$ is the annual exceedance probability of earthquake in k^{th} cell, $m(u_o, D_k)$ is the magnitude in kth source cell that would produce an PGA of u_o or larger at the site and D_k is the distance between site and source cell. To calculate the probability on the basis expected number of the earthquake we use the Gutenberg-Richter (G-R) frequency-magnitude relations: $\mathbf{Log\ N(M) = a - bM}$, where N is the cumulative number of earthquakes with a magnitude greater than M occurring in a specified area and time, and a and b are constants. Hence, in order to calculate the probability of the expected earthquakes of certain magnitudes, we need the b-value, which we derive from the earthquake catalog data. The function $m\ (u_o, D_k)$ is the attenuation relation, which will be discussed in the next section.

We can determine the b value in two ways. First, we can calculate the regional b-value (constant b-value) from seismicity of the entire studied region. Fig. 8 depicts that the general b-value for the region is about 1.00 to 1.14. Second, we can calculate variations of the b values based on local seismicity, such as shown in Fig. 9.

The probability distribution of PGA at the site/region was determined by integrating the influences of the surrounding source cells, i.e.,

$$P(u \geq u_0) = 1 - \prod(1 - P_k(u \geq u_0)) \tag{2}$$

By using an attenuation relationship then we could obtain

$$P(u \geq u_0) = 1 - \prod e^{(-v_i(\geq m(u_0, D_k)))} = 1 - e^{-\sum v_i(\geq m(u_0, D_k))} \tag{3}$$

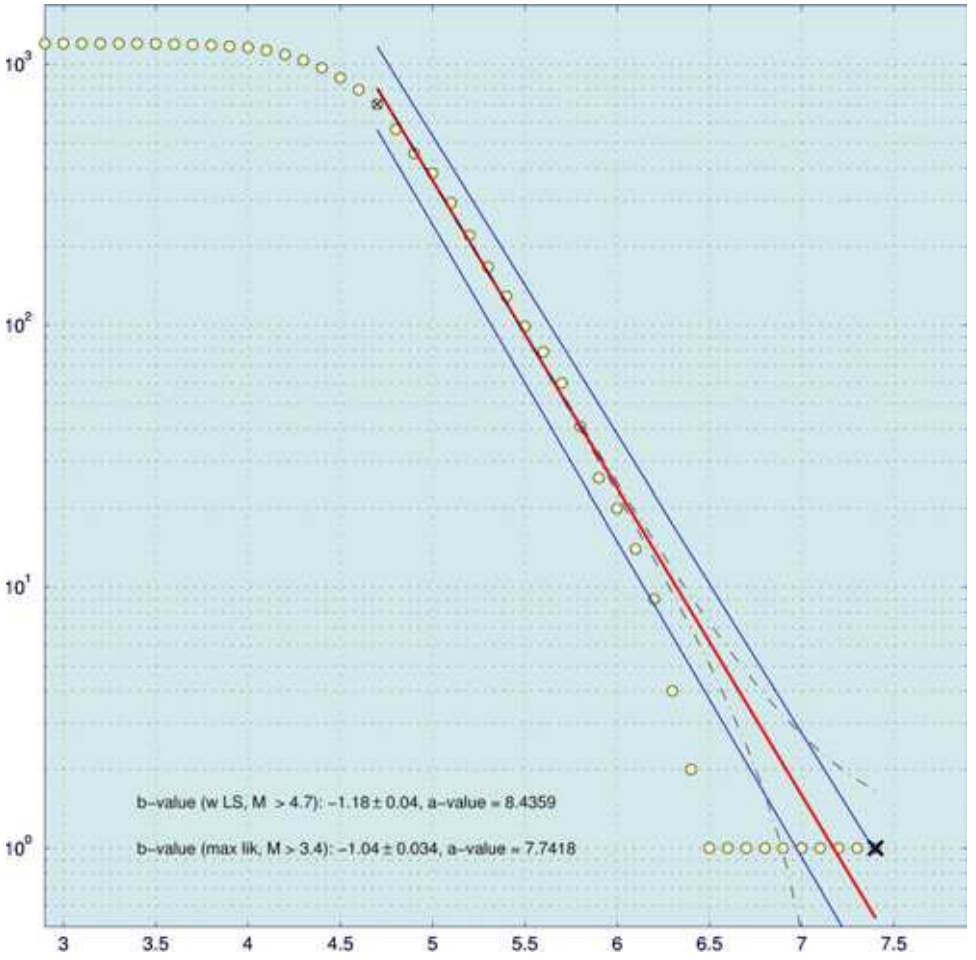

Fig. 8. General b-value for the SFZ from 3S north. Dots are are derived from the seismicity from 1964 to 2005 [updated catalog of Engdahl *et al.*, 1998]. The general b-value is about 1.04 to 1.18.

which gives the annual exceedance probability of particular PGA. For specific time duration T the probability of exceedance is given by

$$P(\mathrm{u} \geq \mathrm{u}_0) = 1 - (1 - \mathrm{P}(\mathrm{u} \geq \mathrm{u}_0))^{\mathrm{T}} = 1 - \mathrm{e}^{-\mathrm{T} \sum \mathrm{v_i}(\geq \mathrm{m}(\mathrm{u}_0, \mathrm{D_k}))} \tag{4}$$

The annual probability of exceeding specified ground motions is calculated by applying Eq. (3) for each grid. For specified time duration, T the probability of exceeding specified ground motions is calculated by using Eq. (4).

5.4. *Results of PSHA*

The seismic hazard assessment is fundamentally an attempt to forecast the likelihoods and effects of earthquakes in the years to come. As such, it is a subject

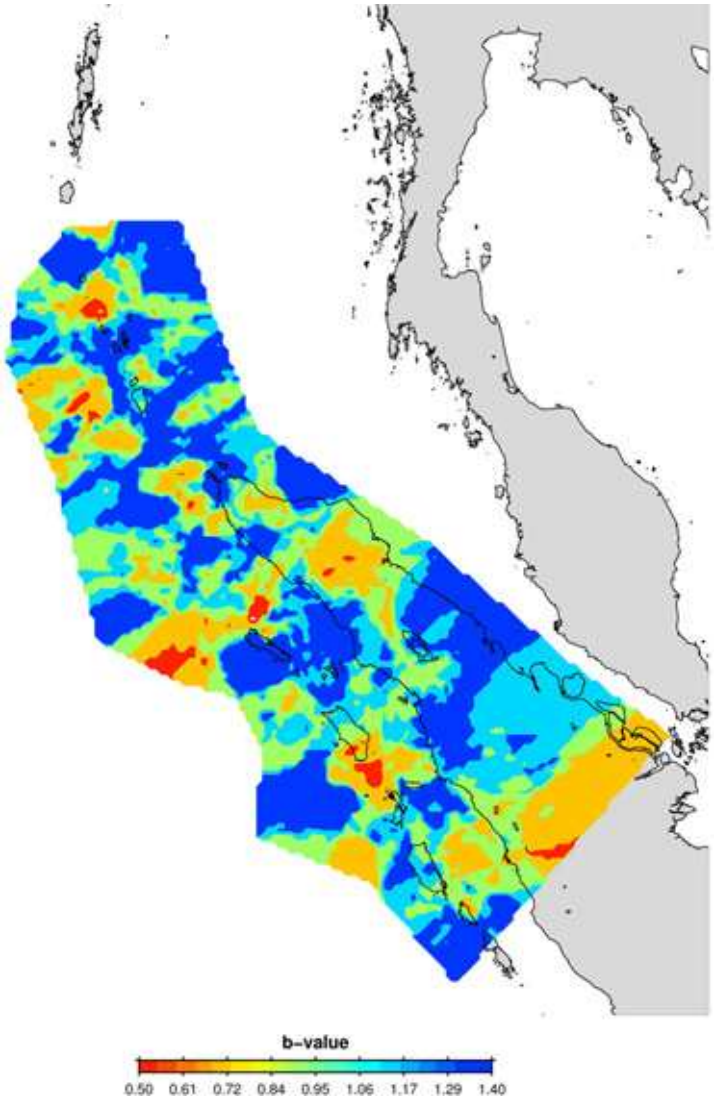

Fig. 9. Map showing b-value variations based on seismicity from 1964 to 2005 of *updated catalog of* Engdahl *et al.* [1998].

to all uncertainties and frailties of any predictive sciences. Sources of uncertainties are inherited from the dynamic natures of earthquakes, limited data on source parameters, surface and subsurface geological condition of the studies areas, and assumptions used in the method. Hence, the PSHA results can be developed in many ways with certain assumptions. However, in this paper, we do not attempt to give an exhausted account of the PSHA works but rather simply show a glimpse of what PSHA can do.

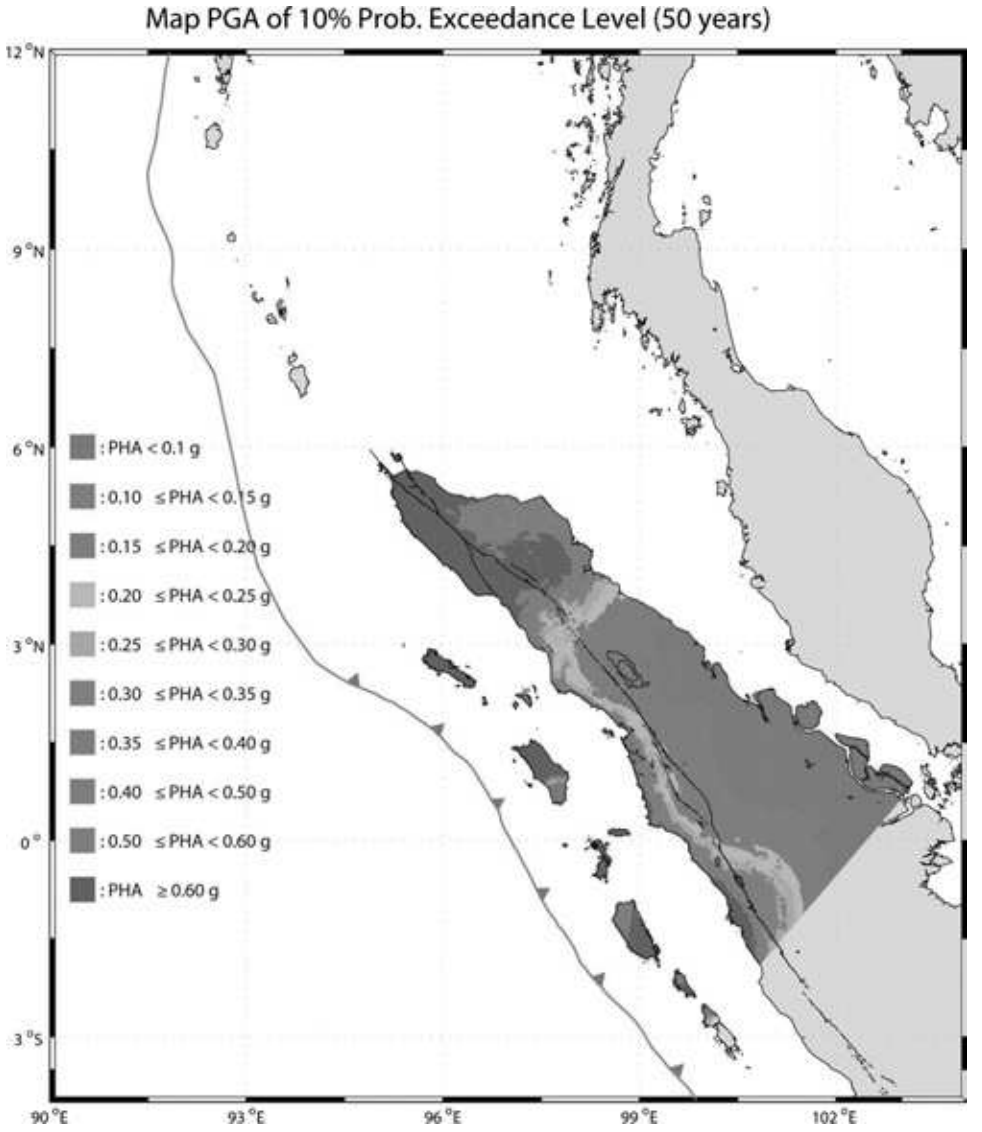

Fig. 10. Map of PGA values for Probability of Exceedance equal to 10% using local variations in b-values displayed in Fig. 7 and taking into account site effects (geological conditions).

For this exercise, we use the b-value variations such as depicted in Fig. 8. To take into account the site effects, we utilize surficial geological map 1:250,000 scale published by ESDM (Dept. Energy and Mineral Resources) to generally estimate shear-wave velocities based on the age of sediments. Then, we use these shear wave values to alter attenuation function. For the on-land seismic sources, we use active fault data of the SFZ as described in Table 1, and for the subduction megathrust segments, we use seismic sources of recent and historical earthquakes from

Table 3. The Sumatran megathrust's major segments. Data are derived from Subarya *et al.* [2006], Briggs *et al.* [2006], Natawidjaja *et al.* [2004], Natawidjaja *et al.* [2006].

Segment	Length (km)	Dip(°)	Depth Down-dip (km)	Average displ. (m)	Effective Convergence rate (mm/yr)	Rec. Int.(yr)	Historical Earthquakes
Aceh-Andaman	1500	12–17	30	15–25	14–34	> 500	2004 (Mw 9.15), 1881 (Mw.), 1941 (Mw.)
Nias-Simelue	400	12–15	35	8–12	40	200–360	1861 (M 8.5), 1907(M 7.8), 2005(Mw 8.7)
Batu	65	12	30	3	15–20	150–200	1935 (Mw 7.7)
Mentawai	670	12	35–50	10–12	40	200–300	1833 (Mw 8.9–9.0), 1797 (Mw 8.4–8.7)

Subarya *et al.* [2006], Briggs *et al.* [2006], Natawidjaja *et al.* [2004, 2006] as shown in Table 3. The result of PSHA is presented in terms of the estimation of expected level of PGA for the probability exceedance of 10% for 50-year period (Fig. 10). We have not considered elapsed times of earthquakes of each fault segment. So, this PSHA map is not time dependent.

6. Effects of Recent Megathrust Events on Sumatran Fault Zone

After the rapid-fire failures of the Aceh-Andaman 2004 (M_w 9.2) and Nias-Simelue 2005 (M_w 8.7) megathrust events, one may wonder the possibilities of their triggering effects [Stein, 2002] on the SFZ segments about 100 kilometers from the megathrust's sources. Previous studies have calculated that the stress shadows of these two megathrust's events probably have significant effects to the SFZ as to the unbroken megathrust section in the southern part of the Sumatran subduction zone [McCloskey *et al.*, 2005; Nalbant *et al.*, 2005; Suleyman *et al.*, 2006]. Here, we want to investigate this aspect based on seismicity before and after the megathrust events.

The seismicity from 1973 to the time before the 26 December earthquake (M_w 9.2) clearly shows a seismic gap on the Aceh-Andaman megathrust zone (Fig. 11). Notice that the preceding 2002 event (M_w 7.2) occurred in Simelue Island, which is later known as the transition zone between the 2004 and 2005 megathrust event [Briggs *et al.*, 2006]. On the east side, many small and moderate earthquakes had occurred along the SFZ segments, north of Aceh in the Andaman Sea region. Other earthquake clusters were also occurring on the middle of the Banda Aceh segment [Sieh and Natawidjaja, 2000] at around 4.5°N, and also on Toru segment at around latitude 2°N.

We suspect that the SFZ segments producing small-moderate earthquake clusters are the weaker sections of the SFZ. Similarly, the 2002 event may also rupture the weaker part that separates the stronger Aceh-Andaman and Nias-Simelue patches.

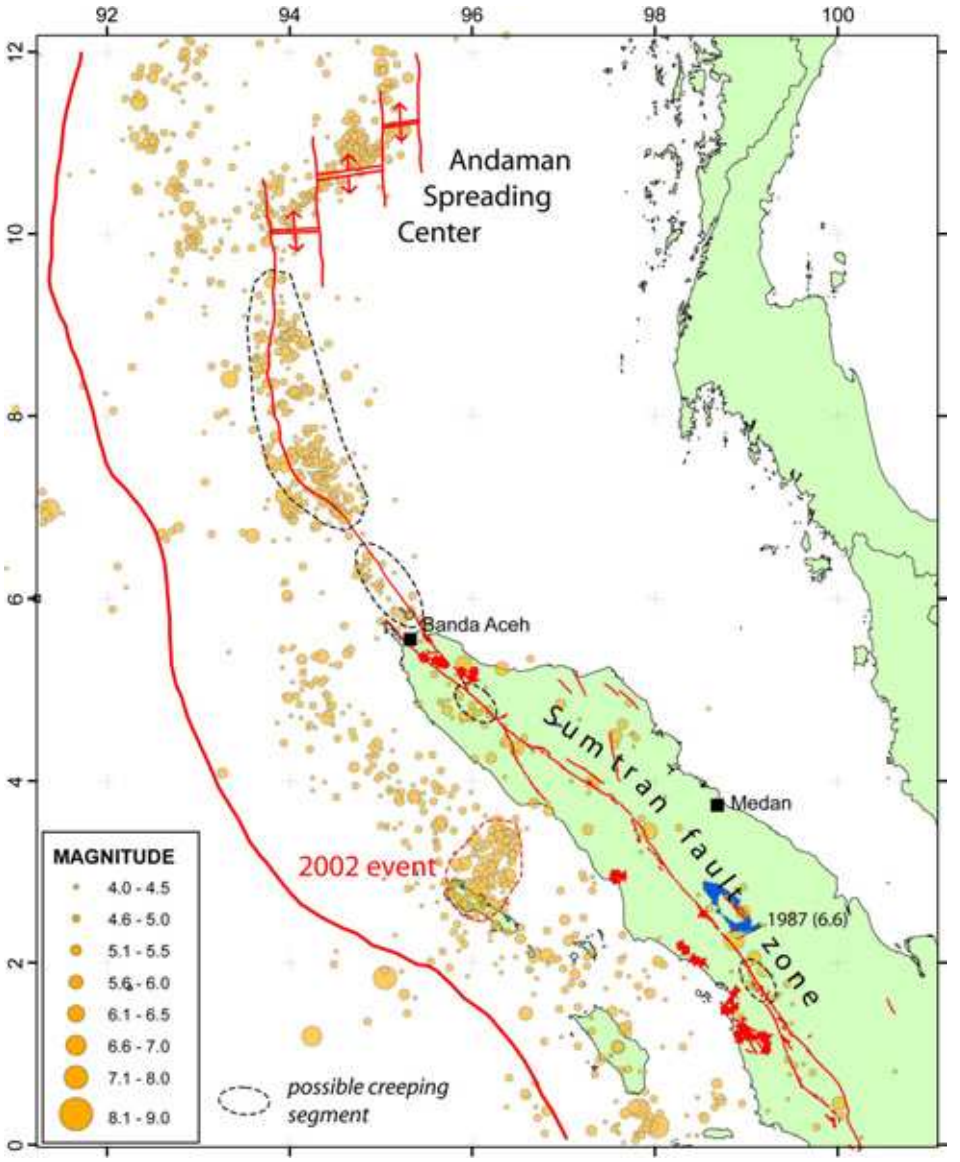

Fig. 11. Seismicity prior to the 26 December 2004 event (M_w 9.2) clearly shows the pre-existing seismic gap on the Sumatran-Andaman megathrust zone. Small-earthquake clusters occurred along suspected weak sections of Sfz north of Equator.

The Aceh-Andaman 2004 event broke the pre-existing seismic gap as marked by the distributions of its aftershocks (Fig. 12). Just in Days, weeks, and months after the 2004 mainshock, many small earthquakes tears the SFZ segments between the Banda Aceh and the Andaman spreading center as well as the suspected weak section in the middle of the Banda Aceh segment. The Nias-Simelue earthquake

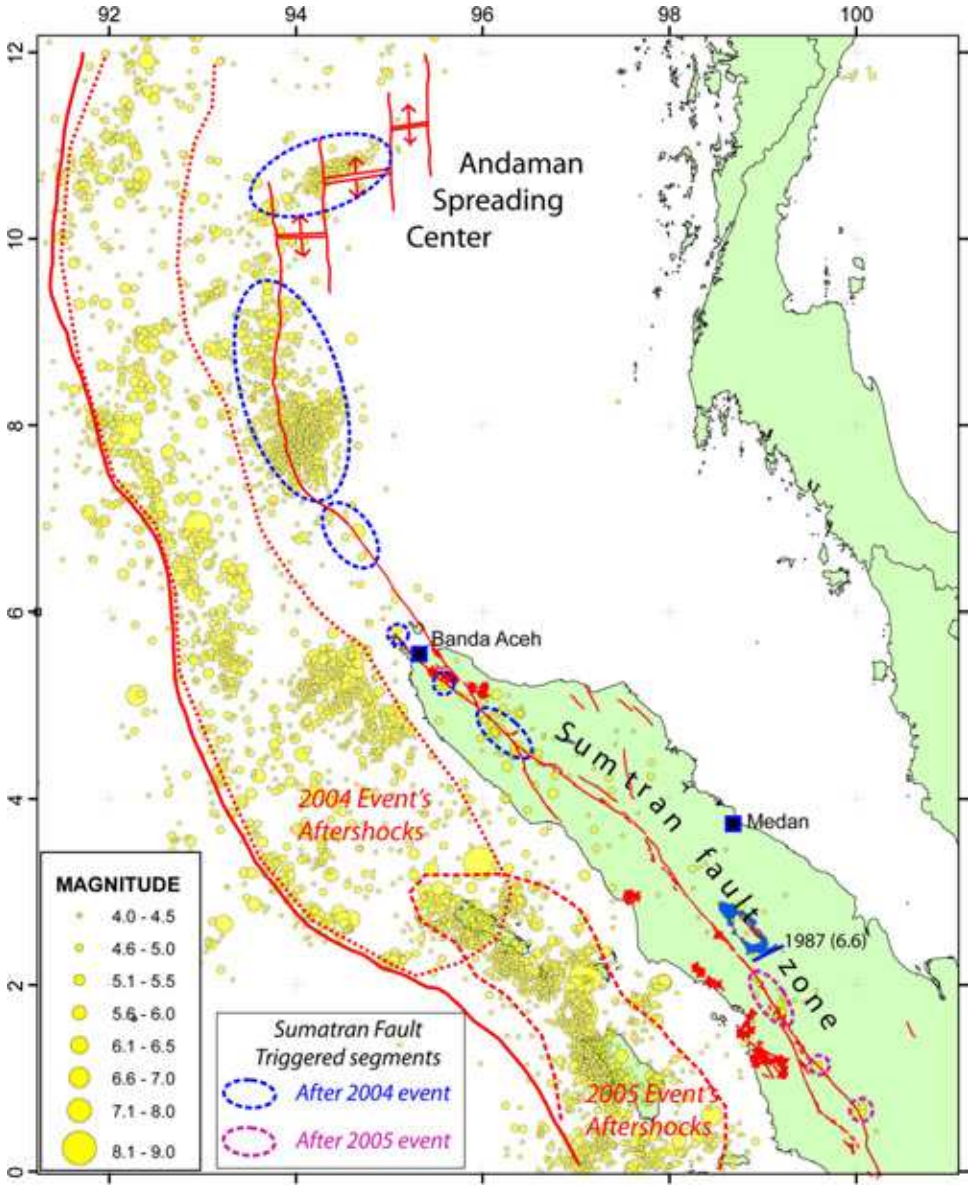

Fig. 12. The 2004 and 2005 megathrust events ruptured the pre-existing seismic gaps and triggered small earthquake clusters on the suspected weak sections of SFZ north of Equator.

ruptured the pre-existing seismic gap in this region. Similarly, in days and weeks after the 2005 event (M_w 8.7) the small-earthquake cluster occurred on the suspected weak Toru segment. Two smaller earthquake clusters also occurred on the Barumun segment at around latitude 1°N (Fig. 12).

Thus, in a crude sense, it seems that the megathrust events did triggere the weak sections of the SFZ. Then, one may pose a question whether this triggering effect could lead to the failure of the strong fault sections in between these weak sections. The historical record tells us that the remaining sections of the Banda Aceh segment and the Seulimeum segment as well as the Renun – Tripa segments may have accumulated enough strain to unleash future earthquakes with magnitude M6.5 to more than M7.5. To anticipate potential future disasters associated with mature strain accumulations and triggering effects of the recent megathrust events, one will need to conduct further investigation on the SFZ north of Equator.

7. Concluding Remarks

The modern map of active fault zones in Sumatra had been constructed on a scale that is large enough to be used in seismic hazard assessments. Geological structures have controlled the past earthquake ruptures and hence are likely to govern future rupture dimensions. On the dextral Sumatran fault, the geological slip rates were determined at selected sites to test the current kinematics model and be used in estimating the earthquake recurrent intervals. Various fault and seismic hazard assessments can be developed based on the state of arts of the active fault knowledge. First, we must consider the hazards associated with future surface faulting along SFZ and associated landslides and liquefactions. Second, the ground-shaking hazards can be anticipated by constructing appropriate deterministic and probabilistic seismic hazard assessments.

Acknowledgment

This research was supported by Indonesian International Joint Research Program (RUTI) grant, National Science Foundation (NSF), Tectonic Observatory Caltech, and Geotechnology Research Center of Indonesian Institute of Sciences (LIPI).

References

Bellier, O., M. Sebrier, M., S. Pramumijoyo, T. Beaudouin, H. Harjono, I. Bahar, O. Forni (1997). Paleoseismicity and seismic hazard along the Great Sumatran Fault (Indonesia). *Journal of Geodynamics*, **24**, 169–183.

Berlage, Jr., H. P. (1934). Ardbeving van Zuid Sumatra van 25 Juni 1933, waar-nemingen in het epicentrale gebied. *Natuurk. Tijdschr.v. Ned. Ind.*, **94**, 15–36.

Briggs, R., K. Sieh, A. Meltzner, D. H. Natawidjaja, J. Galetzka, B. Suwargadi, Y.-J. Hsu, M. Simons, N. Hananto, I. Suprihanto, D. Prayudi, J.-P. Avouac, L. Prawirodirdjo and Y. Bock (2006). Deformation and slip along the Sunda megathrust during the giant Nias-Simeulue earthquake of March 2005, *Science*, 31 March.

Curray, J., D. Moore, L. Lawver, F. Emmel, R. Raitt, M. Henry and R. Kieckhefer (1979). Tectonics of the Andaman Sea and Burma, *AAPG Mem.*, **29**, 189–198.

Cameron, N *et al.* (1983). Geology of the Takengon quadrangle, Sumatra, report Geol. Res. and Dev. Cent., Bandung, Indonesia.

Detourbet, C., O. Bellier and M. Sebrier (1993). La caldera volcanique de Toba et le systeme de faille de Sumatra (Indonesia) vue par SPOT, C. R. Acad. Sci., Ser. II, 316, 1439–1445.

Diament, M., H. Harjono, K. Karta, C. Deplus, D. Dahrin, M. T. Zen Jr., M. Gerard, O. Lassal, A. Martin, and J. Malod (1992). Mentawai fault zone off Sumatra: A new key to the geodynamics of western Indonesia, *Geology*, **20**, 259–262.

Durham, J. (1940). Oeloe Aer fault zone, Sumatra, *Bull. Am. Assoc. Pet Geol.*, **24**, 359–362.

Engdahl, E., R. van der Hilst and R. Buland (1998). Global teleseismic earthquake relocation with improved travel times and procedures for depth determination. *Seismol. Soc. Am. Bull.*, **88**, 722–743.

Fitch, T. J.(1990). Plate convergence, transcurrent faults, and internal deformation adjacent to southeast Asia and the western Pacific, *J. Geophys. Res.*, **77**, 4432–4462.

GSHAP (1999). The Global Seismic Hazard Assessment Program (GSHAP) 1992–1999, *Annuali di Geofisica, Summary Volume Edited by D. Giardini*, 957–1230.

Fukushima, Y. and T. Tanaka (1990). A new Attenuation Relation for Peak Horizontal Acceleration of Strong Earthquake ground motion in Japan. *Seis. Soc. of Amer. Bull*, **V.80**, 757–783.

Genrich, J. F., Y. Bock, R. McCaffrey, L. Prawirodirdjo, C. W. Stevens, S. S. Puntodewo, C. Subarya and S. Wdowinski (2000). Distribution of slip at the northern Sumatran fault system. *Journal of Geophysical Research* **105**, 28,327–28,342.

Hanks, T. C. and H. Kanamori (1979). A moment magnitude scale. *J. Geoph. Res.* **84**, 2348–2350.

Hanks, T. C. and W. H. Bakun (2002). A Bilinear Source-Scaling Model for M–log A Observations of Continental Earthquakes. *Bull. Seism. Soc. Am.* **92**, 1841–1846.

Harjono, H. and D. H. Natawidjaja (2003). Geologi Selat Sunda. In *Proceeding of One-day Seminar "Semiloka Infrastruktur Lintas Selat Sunda". 27 February. ITB, The 44th Universary of ITB.*

Harris, R. and S. Day (1993). Dynamics of fault interaction: Parallel strike-slip faults, *J. Geophys. Res.*, **98**, 4461–4472.

Harris, R., R. Archuleta and S. Day (1991). Fault steps and the dynamic rupture process: 2-D numerical simulations of a spontaneously propagating shear fracture, *Geophys. Res. Lett.*, **18**, 893–896.

Huchon, P. and X. Le Pichon (1984). Sunda Strait and central Sumatra fault, Geology, 12, 668–672.

Katili, J. and F. Hehuwat (1967). On the occurrences of large transcurrent faults in Sumatra, Indonesia. *J. Geosci., Osaka City Univ.*, **10**, 5–17.

Kraeff, A (1952). The earthquake of the Tes region, Benkulen residency on March 15th. *Berita Gunung Berapi*, **1**, 40–56.

Larson, K., J. T. Freymueller and S. Philipsen (1997). Global plate velocities from the Global Positioning System, *J. Geophys. Res.*, **102**, 9961–9981.

Lassal, O., P. Huchon and H. Harjono (1989). Extension crustale dans le detroit de la Sonde (Indonesie): Donnees de la sismique reflexion (campagne Krakatau), *Geophysics*, **309**(2), 205–212.

Megawati, K., Tso-Chien-Pan and K. Koketsu (2003). Response spectral attenuation relationships for Singapore and the Malay Peninsula due to distant Sumatran-fault earthquake, *Earthquake Engineering and Structural Dynamics*, **32**, 2241–65.

McCaffrey, R. (1991). Slip vectors and stretching of the Sumatran fore arc, *Geology*, **19**, 881–884.

McCaffrey, R. (1992). Oblique plate convergence, slip vectors, and forearc deformation, *J. Geophys. Res.*, **97**, 8905–8915.

McCloskey, J., S. S. Nalban and S. Steacy (2005). Earthquake risk from co-seismic stress. *Nature* 434.

Muller, J. (1895). Nota betreffende de verplaatsing van eenige triangulatie pilaren in de redidentie Tapanuli tgv. De aardbeving van 17 Mei 1892. *Natuurk. Tijdschr.v. Ned. Ind.*, **54**, 299–30.

Nalbant, S., S. Steacy, K. Sieh, D. Natawidjaja and McCloskey, J. Earthquake risk on the Sunda trench, *Nature*, **435**, 756–757, 2005.

Natawidjaja, D. H., K. Sieh, S. Ward, H. Cheng, R. L. Edwards, J. Galetzka, and B. W. Suwargadi, 2004. Paleogeodetic records of seismic and aseismic subduction from central Sumatran microatolls, Indonesia, *Journal of Geophysical Research*, 109(B4): **4306**, 1–34.

Natawidjaja, D *et al.* (2006). The giant Sumatran megathrust ruptures of 1797 and 1833: Paleoseismic evidence from coral microatolls, Journal of Geophysical Research.

Natawidjaja, D. H. (1997). Tectonics of the Sunda Strait. *Unpublished research for Ph.D proposition, Caltech.*

Natawidjaja, D. H. and K. Sieh (1994). Slip rates along the Sumatran transcurrent fault and it's tectonics significance. *Abstract in Proceeding on Tectonic Evolution of Southeast Asia*, *Geol. Soc. of London*, 7–8 December, p. 38.

Natawidjaja, D., Y. Kumoro and J. Suprijanto (1995). Gempa bumi tektonik di daerah Bukit tinggi — Muaralabuh: Hubungan segmentasi sesar aktif dengan gempa bumi tahun 1926 dan 1943. *Proceeding of Annual Convention of Geoteknologi-LIPI*, Bandung, Indonesia.

Newcomb, K. and W. McCann (1987). Seismic History and Seismotectonics of the Sunda Arc. *J. Geophys. Res.*, **92**, 421–439.

Petersen, M. D., Dewey, J., Hartzel, S *et al.* (2004). Probabilistic Seismic Hazard Analysis for Sumatra, Indonesia and Across the Southern Malaysian Peninsula. *Tectonophysics*, **390**, 141–158.

Plafker, G., G. Ericksen and C, Fernandez (1971). Geological aspects of the may 31, 1970, Peru earthquake. *BSSA* **61**, 543–178.

Prawirodirdjo, L., Y. Bock, J. F. Genrich, S. S. O Puntodewo, J. Rais, C. Subarya and S. Sutisna (2000). One century of tectonic deformation along the Sumatran fault from triangulation and Global Positioning System surveys. *Journal of Geophysical Research*, **105**, 28,343–28,363.

Research Group for Active Faults, Main Active Faults in and Around Japan, University of Tokyo Press, Tokyo, 1980.

Reid, H.(1913). Sudden earth movements in Sumatra in 1892, Bull. Seismol. Soc. of Am. Bulletin, **3**, 72–79.

Saroglu, F., O. Emre and I. Kuscu (1992). Active fault map of Turkey, Gen. Dir. of Miner. Res. and Explor. (MTA), Ankara, Turkey.

Sieh, K., Y. Bock and J. Rais (1991). Neotectonic and paleoseismic studies in west and north Sumatra. *EOS Trans. AGU 72(44), Fall Meet. Suppl.*, 460.

Sieh, K. and Natawidjaja, D. (2000). Neotectonics of the Sumatran fault, Indonesia. *Journal of Geophysical Research*, **105**, 28,295–28,326.

Sieh, K., J. Zachariasen, Y. Bock, L. Edwards, F. Taylor, P. Gans P. (1994). Active tectonics of Sumatra. *GSA Abstracts with Programs 26, No. 7, Sept.*

Stein, R. (2002). Earthquake conversations. *Scientific American.*, January volume, 73–79, 2002.

Suleyman, N., J. McCloskey, K. Sieh, S. Steacy and D. H. Natawidjaja (2005). Stress interaction and the 2004/2005 earthquakes. *Abstract in Proceeding AGU Fall Meeting*, San Fransisco.

Subarya, C., M. Chlieh, L. Prawirodirdjo, J. P. Avouac, Y. Bock, K. Sieh, A. Meltzner, D. Natawidjaja and R. McCaffrey (2006). Plate-boundary deformation associated with the great Sumatra–Andaman earthquake: *Nature, p. doi: 10.1038/nature04522*

Tapponnier, P. and P. Molnar (1977). Active faulting and tectonics in China, *J. Geophys. Res.*, **82**, 2905–2930, 1977.

Untung, M., N. Buyung, E. Kertapati, Undang and C. Allen (1985). Rupture along the Great Sumatran fault, Indonesia, during the earthquakes of 1926 and 1943. *Bull. Seismol. Soc. Am.*, **75**, 313–317.

Visser, S. (1927). De aardbevingen in de Padangse Bovalanden, Natuurwet. *Tijdschr. Ned. Indie.*, **87**, 36–71.

Visser, S. (1922). Inland and submarine epicentra of Sumatra and Java earthquakes. *Koninklijk Magnetisch en Meteorologisch Observatorium te Batavia*, **9**, 1–14.

Wells, D. L. and K. J. Coppersmith (1994). New empirical relationships among magnitude, rupture length, rupture width, rupture area, and surface displacement. *Bull. Seism. Soc. Am.* **84**, 974–1002.

Wichmann, A. (1918). Die erdbeben des Indischen Archipels bis zum Jahre 1857. *in Afdeling Natuurkunde Nderlandse Verhandelingen, 193 pp.,* Kon Akademie van Watenschapen, Amsterdam (English translation).

Wichmann, A. (1918). Die erdbeben des Indischen Archipels von 1858–1877. *in Afdeling Natuurkunde Nderlandse Verhandelingen, 209 pp.*, Kon Akademie van Watenschapen, Amsterdam (English translation).

Widiwijayanti, C., J. Deverchere, R. Louat, H. Harjono, M. Diament and D. Hidayat (1996). Analysis of the aftershock sequence of the M_w 6.8 Liwa earthquake, Indonesia. *Geophys. Res. Lett.*, **23**, 3051–3054.

Working Group on the Probabilities of Future Large Earthquakes in southern California (1995). Seismic Hazards in Southern California: Probable earthquakes, 1994–2024. *Bulletin of Seismological Society of America*, **85**(2), 379–439.

Yeats, R., K. Sieh and C. Allen (1997). The Geology of Earthquakes, 568 pp., Oxford University Press, New York.